

Sintering and grain growth of ultrapure alumina

SO IK BAE, SUNGGI BAIK

Department of Materials Science and Engineering, Pohang Institute of Science and Technology (POSTECH), Pohang, 790-600, Korea

The kinetics of densification and grain growth of ultrapure alumina ($> 99.999\%$) were measured for clean sintering conditions in a pure-sapphire tube, and compared with kinetics measured during normal sintering conditions in an alumina crucible of 99.8% purity. For the clean condition, the microstructure of sintered alumina remained homogeneous and only normal grain growth was observed up to 1900°C for 5 h. However, under the normal sintering condition, both normal and abnormal grain growth were observed depending on the sintering temperature and time. Thus, abnormal grain growth in alumina could be effectively suppressed without introducing sintering aids (such as MgO) by using an ultrapure powder and by preventing the introduction of any impurities throughout the sintering process. This result strongly suggests that abnormal grain in commercially pure alumina ($\leq 99.99\%$) is not an intrinsic property of alumina but an extrinsic property controlled by minor constituents that can be present in the original powder or introduced during powder processing and subsequent sintering.

1. Introduction

In recent years, research [1-8] has focused on understanding the effects of minor chemical constituents on the sintering of alumina. It has been determined that MgO is a beneficial sintering aid [1-4], while CaO and SiO₂ have a deleterious influence on the sintering of alumina [6-8]. However, the detailed role of these constituents in the sintering process is still controversial. This controversy is partly because the amount of impurities in alumina powder varies widely depending on its fabrication history, the cleanliness of powder-processing procedures, and sintering conditions [9]. Commercial-purity alumina powders typically contain several thousand parts per million (p.p.m.) of impurities. Impurities may also be introduced during powder processing and during firing. Since the level of MgO added to control abnormal grain growth is also typically in the range of several hundreds to thousands of parts per million, a great deal of caution is needed in interpreting the influence of impurities in the presence of MgO.

Previous experimental results indicate that abnormal grain growth in commercially pure alumina is strongly correlated with the presence of impurities, most notably CaO and SiO₂ which have often been found, particularly in the grain boundaries. Bennison and Harmer [3] reported that MgO doping inhibited grain growth in fully dense alumina and that the degree of inhibition depends on the purity of the starting powder. Kaysser *et al.* [6] demonstrated that the presence of an intergranular liquid phase (anorthite) induces grain faceting and leads to a more tabular grain morphology, which would eventually lead to abnormal grain growth. Handwerker *et al.* [7]

showed experimental evidence that chemical inhomogeneities in the starting powders are more responsible for abnormal grain growth in alumina than morphological inhomogeneities such as large grains or hard agglomerates. Recently, Baik and Moon [8] demonstrated that the beneficial effect of MgO might be related to its effectiveness in controlling the segregation behaviour of Ca ions to pore surfaces and grain boundaries.

It becomes interesting to see whether abnormal grain growth can be suppressed totally by avoiding all impurities throughout the fabrication procedure. If it can, then how much CaO and/or SiO₂ are required for triggering abnormal grain growth, and what is the minimum amount of additional MgO required to suppress the abnormal grain growth as a function of the amount of CaO and/or SiO₂ added initially? The purpose of this paper is to answer the first question experimentally by investigating the kinetics of the sintering and grain growth of ultrapure alumina with a purity that exceeds 99.999%. Powder processing and sintering were performed under carefully prepared clean conditions. No evidence was found of abnormal grain growth under such conditions. However, sintering under a less clean condition induced extensive abnormal grain growth.

2. Experimental procedure

Samples were prepared from ultrapure α -alumina powder (AKP5N, average particle size 0.3 μm) for which the manufacturer (Sumitomo Chemical Company, Osaka, Japan) claimed a 99.999% purity. The chemical data provided by the manufacturer show

that total cationic impurities are less than 10 wt p.p.m. with individual impurities such as Na, Ca, Si, Fe, and Cu being less than 1 wt p.p.m. each. The alumina powder was initially dispersed in absolute ethyl alcohol (HPLC grade, Aldrich Chemical Company, Incorporated, Milwaukee, WI, USA) using polyethylene bottles, and dried at 70 °C for 48 h. The powder was cold pressed into disks using stainless-steel die and isostatically pressed at $2.0 \times 10^7 \text{ kg m}^{-2}$ in a rubber bag. The as-received powder was highly agglomerated. The green densities were about 42% of the theoretical density. The surface layer of green bodies was scraped off using a thin sapphire plate prior to sintering to remove possible contamination during die pressing.

Sintering was conducted under flowing Ar gas in a furnace (M60, Centorr Associates, Incorporated, Suncook, NH, USA) heated with tungsten elements. The specimens were heated at a constant rate of $15^\circ\text{C min}^{-1}$ up to the sintering temperature. Two different sintering conditions were adopted. First, the sample was loaded on a sapphire tube covered loosely at both ends with sapphire disks (the clean sintering condition). Secondly, the sample was placed in a commercial-purity alumina crucible (99.8%) with a thin layer of the ultrapure alumina powder in between so that they were not directly in contact, and then the crucible was covered with a lid (the normal sintering condition).

The densities of sintered bodies were measured to an accuracy of 0.1 kg m^{-3} using Archimedes' method with distilled water as the immersion medium. The samples were ground with successively finer grades of SiC papers, polished with 6, 3, and 1 μm diamond pastes successively, and then thermally etched at 1650 °C for 1 h on a sapphire plate in a flowing Ar gas. The samples were then coated with gold and examined by scanning electron microscopy (SEM). The average grain size was measured by an intercept method and calculated from the relationship, $G = 1.5L$, where G is the average grain size and L is the average intercept length. Approximately 500 intercepts were counted for each sample.

3. Results

The temperature–time regions in which the experiments were conducted are shown in Fig. 1a for the clean sintering condition in a sapphire tube, and in Fig. 1b for the normal condition in an alumina crucible. No evidence was found for abnormal grain growth under the clean sintering condition even after 5 h at 1900 °C; but, for the normal sintering condition, abnormal grain growth was observed even at 1750 °C for sintering times longer than 3 h and at higher temperatures for shorter times. The boundary for the onset of abnormal grain growth is shown in Fig. 1 by a dashed line. This data shows that the time for initiation of abnormal grain decreases as temperature increases.

Microstructural evolution of ultrapure alumina sintered under the clean condition at 1850 °C is shown in Fig. 2. The average grain size increases as the sintering

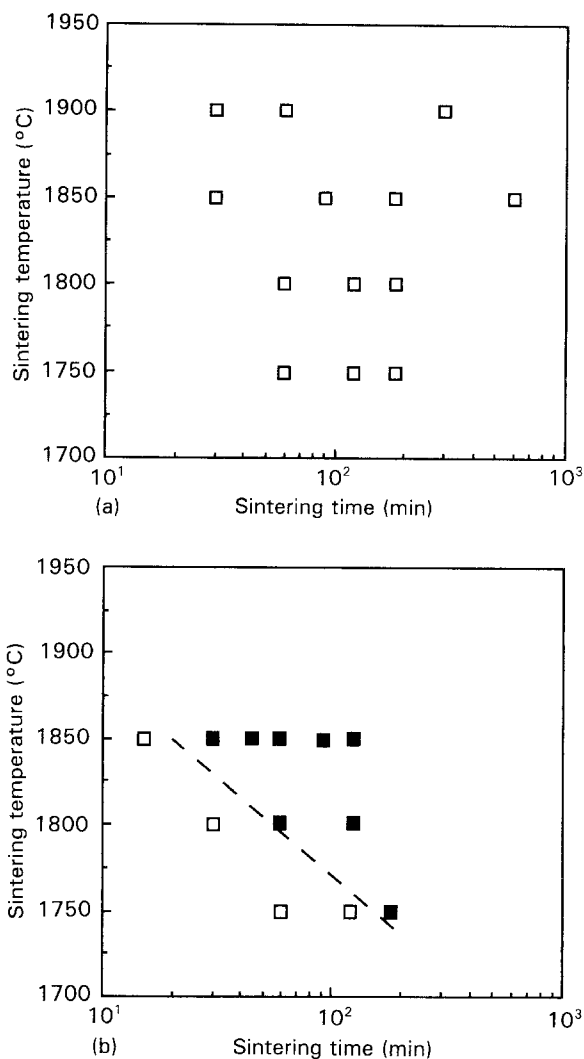


Figure 1 The effect of sintering temperature and sintering time on the initiation of abnormal grain growth for: (a) the clean condition; and (b) the normal condition; (□) normal grain growth, (■) abnormal grain growth, and (---) the boundary for the onset of abnormal grain growth.

time increases, but the grain shape remains quite homogeneous and equiaxed up to the maximum temperature and time tested (1900 °C for 5 h). The majority of pores are located at the grain boundaries with a few isolated pores located within the grains. The shape of the trapped pores is almost spherical. Although some evidence of pore–boundary separation could be observed, no abnormal grain growth could be found.

The SEM micrographs in Fig. 3 show microstructural changes under the normal sintering condition which are drastically different to those under clean sintering at the same temperature, 1850 °C. Until 15 min of sintering there was no sign of abnormal grain growth. However, after sintering for 30 min, large abnormal grains appeared, and the fraction of abnormally large grains increased rapidly as the sintering time increased. The size of abnormal grains after sintering for 180 min ranges up to few hundred micrometres. Some boundaries are highly faceted. The majority of pores are trapped within the large grains.

The density variations with sintering time under the two different sintering conditions are plotted in Fig. 4. The densification rates in the initial and intermediate stage of sintering are much higher for the normal

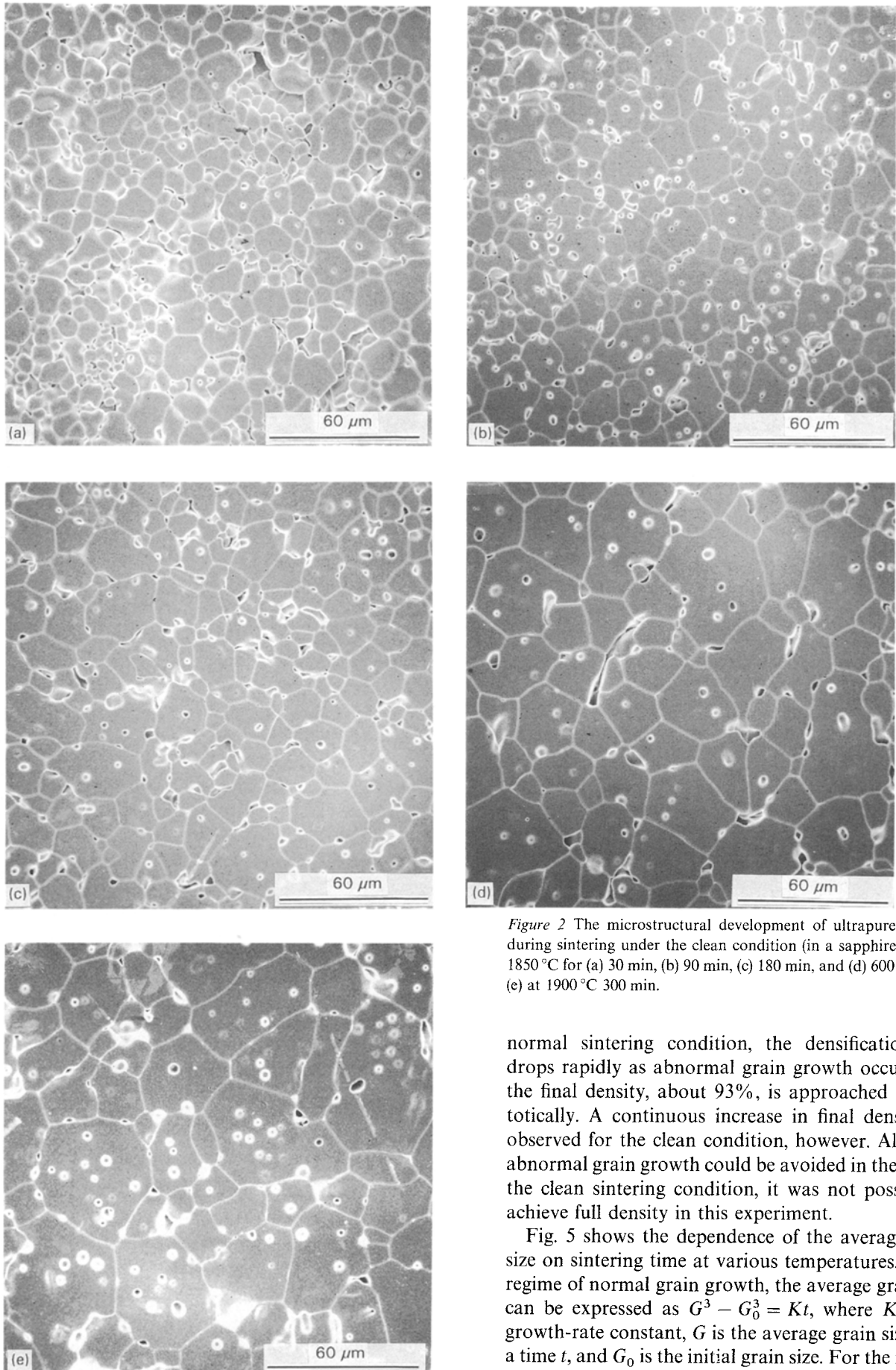


Figure 2 The microstructural development of ultrapure alumina during sintering under the clean condition (in a sapphire tube): at 1850 °C for (a) 30 min, (b) 90 min, (c) 180 min, and (d) 600 min; and (e) at 1900 °C 300 min.

normal sintering condition, the densification rate drops rapidly as abnormal grain growth occurs, and the final density, about 93%, is approached asymptotically. A continuous increase in final densities is observed for the clean condition, however. Although abnormal grain growth could be avoided in the case of the clean sintering condition, it was not possible to achieve full density in this experiment.

Fig. 5 shows the dependence of the average grain size on sintering time at various temperatures. In the regime of normal grain growth, the average grain size can be expressed as $G^3 - G_0^3 = Kt$, where K is the growth-rate constant, G is the average grain size after a time t , and G_0 is the initial grain size. For the normal sintering condition, before the abnormal grain growth set in, the normal grain growth followed the same relationship as that for the clean sintering condition; however, the growth rate constant was much higher. For instance, at 1850 °C, K was $1.1 \times 10^{-18} \text{ m}^3 \text{ s}^{-1}$ for

sintering condition than for the clean sintering condition. The densification rate for the normal condition in the density range 85–93% is about 3–5 times higher than that of the clean condition. However, for the

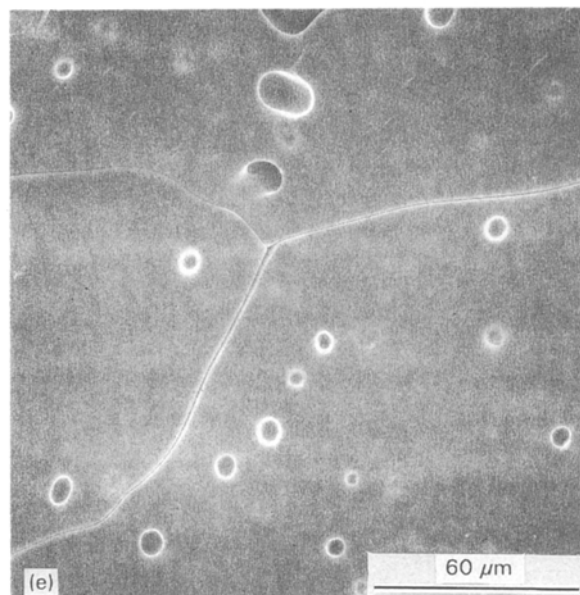
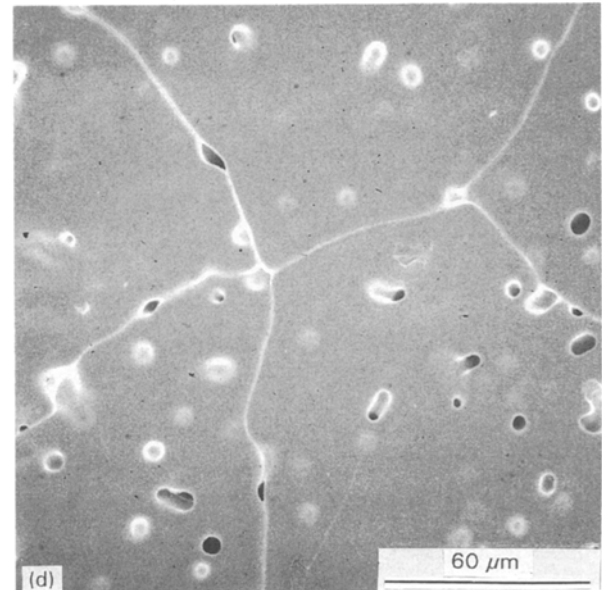
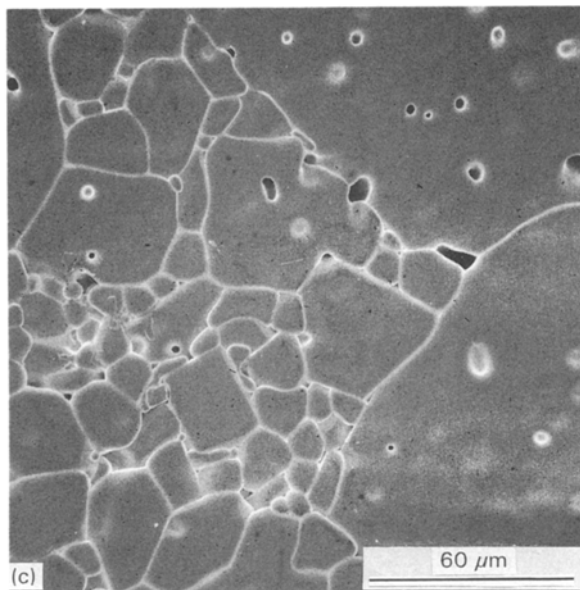
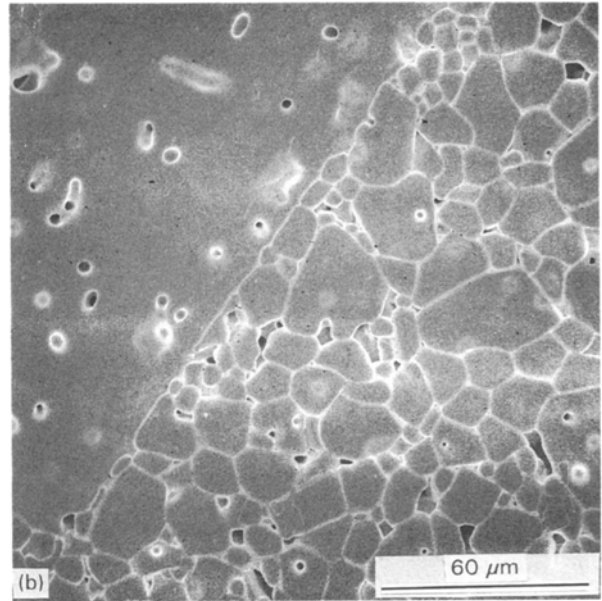
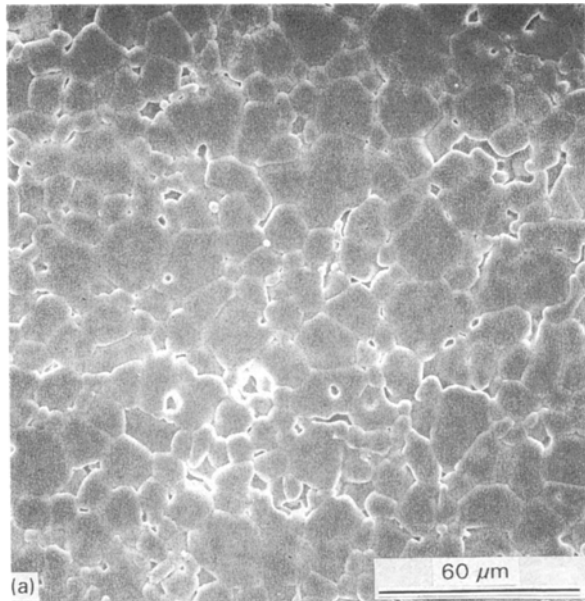


Figure 3 The microstructural changes of ultrapure alumina during sintering under the normal condition (in a 99.8% crucible) at 1850 °C for: (a) 15 min, (b) 30 min, (c) 45 min, (d) 90 min, and (e) 180 min.

ature following the expression, $K = K_0 \exp(-Q/RT)$, where Q is the activation energy for grain growth. The activation energies determined by plotting $\log K$ against homologous temperature were 690 kJ mol^{-1} for the clean sintering condition, and 640 kJ mol^{-1} for the normal sintering condition, as illustrated in Fig. 6.

4. Discussion

It has been demonstrated in an earlier study [8] that the clean sintering condition adopted in this experiment results in the formation of contamination-free grain boundaries after sintering. When the container was changed to the commercial-alumina crucible ($\sim 99.8\%$) in the normal sintering condition, contaminants could be easily transferred from the crucible to the samples being fired. Because the samples were separated from the crucible wall by the ultrapure

the clean condition, and $3.3 \times 10^{-18} \text{ m}^3 \text{ s}^{-1}$ for the normal condition. So the growth-rate constant increases three-fold under normal conditions. The growth rate constant, K , is also dependent on temper-

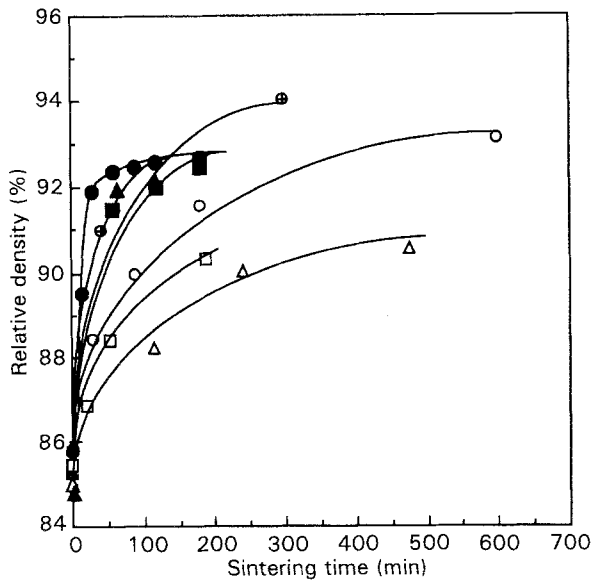


Figure 4 Density versus sintering time and sintering temperature under two different sintering conditions: clean (\oplus , \circ , \square , \triangle) at 1900, 1850, 1800, and 1750°C, respectively; and normal (\bullet , \blacksquare , \blacktriangle) at 1850, 1800, and 1750°C, respectively.

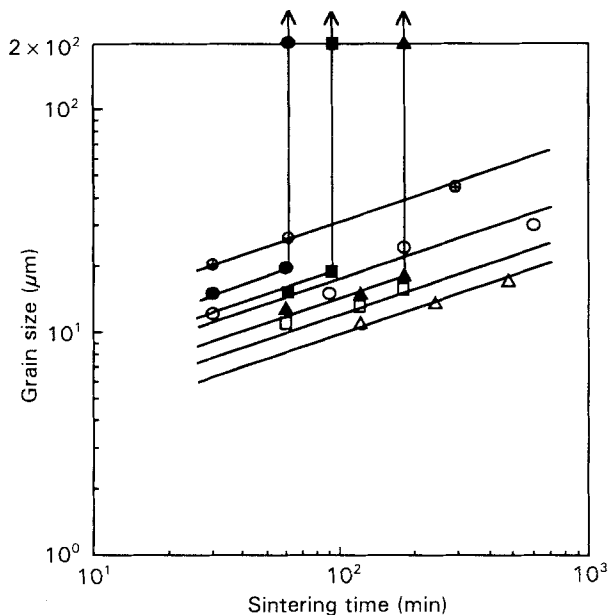


Figure 5 Average grain size versus sintering time at various sintering temperatures. The sizes follow the normal grain growth kinetics $t^{1/3}$ dependence, until abnormal grain growth sets in: clean (\oplus , \circ , \square , \triangle) at 1900, 1850, 1800, and 1750°C, respectively; and normal (\bullet , \blacksquare , \blacktriangle) at 1850, 1800, and 1750°C respectively.

alumina powder, the only possible route for the transfer of contaminants was through the vapour phase. In conventional sintering practice, the furnace wall, the heating element and the heat shield can also be sources of contaminants. However, in this study, the contaminants should be mainly from the alumina crucible. The major impurities present in the crucible ($\sim 99.8\%$) according to the manufacturer are MgO (1000 p.p.m.), Na₂O (300 p.p.m.), and SiO₂ (400 p.p.m.), smaller amounts of FeO and CaO are also present. The vapour pressures of each component up to 1700°C are in the order, Na₂O > SiO₂ > MgO [10]. It has been reported [11] that Na₂O reacted with MgO and Al₂O₃ to form a β''' -alumina phase

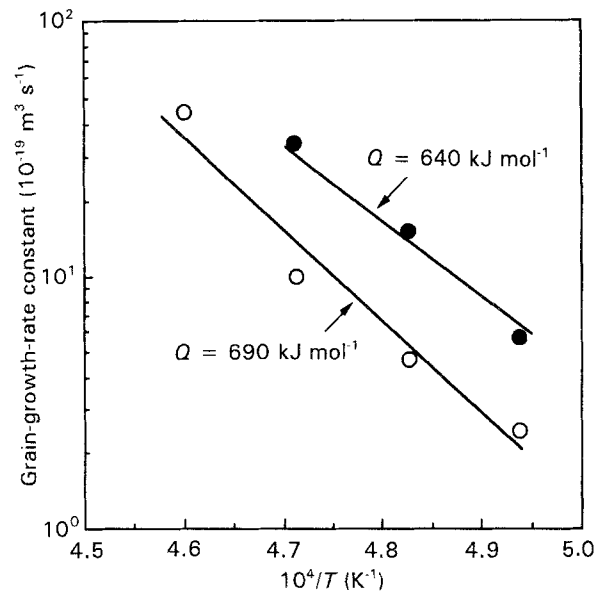


Figure 6 Temperature dependence of the grain-growth-rate constant for two different sintering conditions: (\circ) clean, and (\bullet) normal. The activation energies are calculated from the slopes of the fitted lines. For the normal sintering condition, only the data representing normal-grain-growth behaviour are plotted.

(NaMg₂Al₁₅O₂₅) at elevated temperatures, after which the Na₂O vapour pressure becomes relatively lower. Therefore, the most probable contaminant in our case is SiO₂ which is present in the crucible; it volatilizes easily by the reaction, $2\text{SiO}_2 = 2\text{SiO}\uparrow + \text{O}_2$, and could be transferred to the sample being fired. Simpson and Carter [12] have previously demonstrated that a small amount of SiO₂ and CaO can be transferred to alumina transmission electron microscopy (TEM) samples through a vapour-phase process. CaO is also known to be deleterious and its vapour transfer is also possible. Attempts were made to identify the contaminants by induction coupled plasma (ICP) analysis. Unfortunately, specimens prepared by ICP analysis were even more contaminated and the contaminants introduced during sintering were not identified.

As shown in Figs 2 and 3, the microstructural evolution of ultrapure alumina is quite different under the two different sintering conditions. This result demonstrates convincingly that the impurities taken up during sintering by vapour transfer trigger the premature abnormal grain growth in ultrapure alumina. This result also implies that abnormal grain growth is inevitable in pure alumina during normal sintering practices because it is difficult to avoid the introduction of low-level contaminants from various sources including the original starting powder, powder processing, or sintering.

Now, the pressing questions are; (i) what determines the boundary between the normal- and abnormal-grain-growth regions shown in Fig. 1b? and (ii) what is the role of impurities such as SiO₂ or CaO in the change from the behaviour shown in Fig. 1(a)? The answers to these questions would certainly help in understanding the mechanism that initiates abnormal grain growth in commercial alumina and in understanding the role of MgO in controlling abnormal grain growth.

Fig. 5, in conjunction with the microstructures in Figs 2 and 3, shows that, even though normal grain growth proceeded under the clean condition without any changes in the kinetic constants, sintering at a higher temperature or for a longer time did not lead automatically to abnormal grain growth. Fig. 5 also shows that for the normal condition the grain shape is equiaxed following similar grain-growth kinetics before the onset of abnormal grain growth. Two important points can be derived from these observations: first, the condition of abnormal grain growth is not determined by grain size alone; and secondly, impurities begin to induce abnormal grain growth at a critical grain size. That is, abnormal grain growth appears suddenly at a critical grain size in the presence of impurities. Fig. 5 demonstrates that this critical grain size is in the 15–20 μm range for samples prepared in the normal sintering condition. Therefore, the critical grain size as a condition for abnormal grain growth should be interpreted in its connection to an impurity effect.

The sudden appearance of abnormal grains has been related to grain boundary chemistry. Kaysser *et al.* [6] proposed that a liquid phase appears suddenly since at some critical grain size in the capacity of grain boundaries to keep the concentration of impurities in the grains below the solubility limit is exceeded. The sudden appearance of a liquid can be applied to explain the onset of abnormal grain growth in Fig. 1b. The scenario of impurity incorporation in the normal sintering condition can be understood as follows; at an early stage of sintering, volatile impurities, like SiO_2 , are transferred by gas diffusion to the sample being fired so that they contaminate grain boundaries, grain surfaces, and pores. In theory, this transfer should continue until the impurities reach their solubility limits in the matrix and in the grain boundaries. However, as sintering proceeds and grains grow, the total grain-boundary area is reduced and the impurity concentration in the grain boundaries increases accordingly. At a critical grain size this concentration exceeds the level required for the formation of second phases — in our situation, a liquid phase that has been previously demonstrated to trigger abnormal grain growth in alumina.

The observation of faceting along certain crystallographic planes in abnormal grains (see Fig. 3) supports the argument that impurities introduced during the normal sintering condition form intergranular liquid phases. Correlations among faceted grains, abnormal grain growth, and the presence of liquid phases have been presented by many researchers. Hansen and Phillips [13] reported that in a 99.8% alumina nearly all grain boundaries were coated with a thin layer of amorphous intergranular material which may have induced faceting. Susnitzky and Carter [14] reported that a SiO_2 -deposited boundary in a sapphire bicrystal was flat and faceted along the (0001) plane. Handwerker *et al.* [7] found extensive faceting in alumina containing an anorthite-based liquid phase.

The role of impurities below the critical grain size can be understood from Figs 4 and 5, which show that the densification rate and grain-growth rate were

enhanced when samples were sintered in the normal condition. The activation energies for grain growth, 690 kJ mol^{-1} in the clean sintering condition and 640 kJ mol^{-1} in the normal sintering condition (see Fig. 6), are very close to those reported for Al volume diffusion [15]. Coble [1] reported that the phenomenological activation energy of grain growth for pure alumina was 640 kJ mol^{-1} , which is consistent with our value in the normal sintering condition. A significant point is that the impurities apparently enhance grain-growth kinetics by a factor of three without altering its mechanisms.

It is known [16, 17] that the densification rate (dp/dt) depends on the grain size following the relationship, $dp/dt = CD/G^n$, where C is a constant, D is the diffusion coefficient, G is the grain size, and n is the grain-size exponent. The exponent, n , is 3 for lattice-diffusion-controlled densification and 4 for grain-boundary-diffusion-controlled densification. Fig. 7 illustrates the dependence of densification rate on grain size for two different sintering conditions at 1850°C . Only the data representing normal grain growth behaviour are plotted in Fig. 7. The grain-size exponent calculated from the gradients in Fig. 7 are -2.9 for the clean condition, and -3.5 for the normal condition. The result indicates that lattice diffusion is the dominant densification mechanism under the clean sintering condition, while the densification mechanism under the normal sintering condition is a combination of lattice and grain-boundary diffusion. It has previously been reported in the literature [3, 16, 17] that the grain size exponent n is -3.5 (mixed behaviour) or -4.0 (grain-boundary diffusion) for undoped commercially pure alumina. The divergence may be due to the different purities of the starting powders, initial microstructures, or the range of density measurements. The densification rate at a constant grain size also shows an increase, by a factor

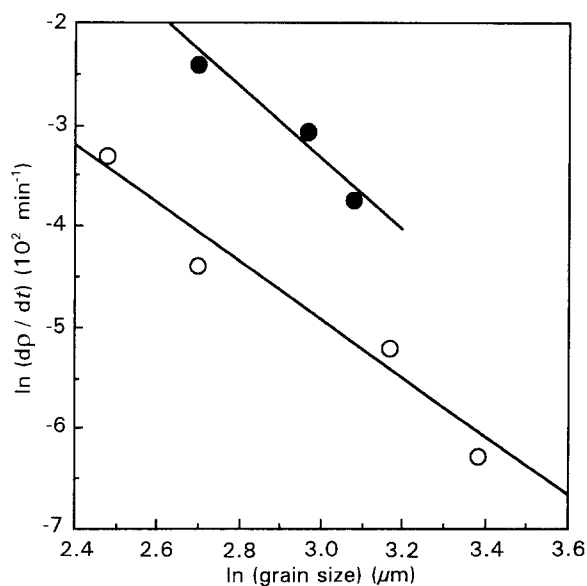


Figure 7 The rate of densification determined from Fig. 4 is plotted against the average grain size measured for a given sintering time at 1850°C : (○) clean sintering, and (●) normal sintering (normal grain growth only).

of 3 to 5, which is presumably due to the presence of impurities.

It can be asked whether ultrapure alumina would exhibit abnormal grain growth if the time and temperature for sintering increase further under the clean condition. If only the morphological aspects of abnormal-grain-growth conditions are considered, it is immediately clear that the clean sintering condition is in fact much more favourable for abnormal grain growth than the normal condition. The density/grain-size trajectory compiled in Fig. 8 clearly proves the point. Bennison and Harmer [3] reported that even fully dense alumina of 99.995% purity showed normal-grain-growth behaviour. Therefore, it is highly unlikely that a simple increase in density or grain size would reach a critical point for abnormal grain growth. As discussed previously, if the critical condition is assumed to be set by the formation of an intergranular liquid phase, the possibility of observing abnormal grain growth can be ruled out under the clean sintering condition.

In summary, this result suggests that the abnormal grain growth may not be an intrinsic property of pure alumina induced by structural anisotropy, but rather an extrinsic property controlled by minor constituents introduced during powder synthesis, processing and sintering. Therefore, abnormal grain growth in alumina could be effectively avoided without introducing sintering aids (such as MgO) by using an ultrapure powder, and sintering while preventing the introduction of any impurities during the sintering process. This contradicts the previous belief that pure alumina cannot be sintered to full density due to abnormal grain growth, and that if abnormal grain growth is suppressed then alumina can be sintered to full density. We found that neither pore-boundary separation, density, nor grain size determined the condition for the initiation of abnormal grain growth. The presence of large agglomerates in the starting powder, and a wide distribution in grain size was not the major factor. This result strongly suggests that the chemical effect is a far more important factor in triggering discontin-

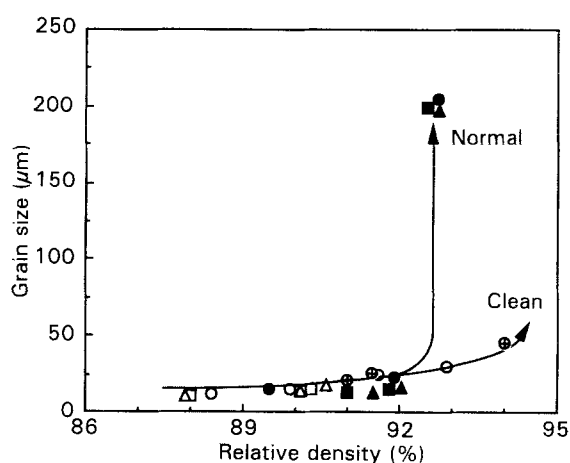


Figure 8 Grain size/density trajectory under two different sintering conditions: clean (⊕, ○, □, △) at 1900, 1850, 1800, and 1750 °C respectively; and normal (●, ■, ▲) at 1850, 1800, and 1750 °C respectively.

uous grain growth in alumina. It is consistent in part with earlier work by Patrick and Cutler [18], Kaysser *et al.* [6] and Handwerker *et al.* [7].

Another important implication of this result is that the effect of MgO additions for the purpose of controlling abnormal grain growth in alumina should be considered within the context of its influence to the critical impurities which are in fact responsible for abnormal grain growth. In recent studies involving one of the authors [8, 19], MgO was found to be effective in suppressing inhomogeneous CaO segregation to the grain boundaries of sintered alumina. It is now interesting to study more carefully the effects of MgO on small amounts of SiO₂ using ultrapure alumina through the use of controlled doping and sintering.

5. Conclusions

The kinetics of densification and grain growth for ultrapure alumina have been studied with a clean sintering condition which provided a contamination-free environment. These results were compared with those obtained for a normal sintering condition that more closely approximates those conditions routinely practised in the laboratory. The results obtained in these two conditions were drastically different and the analysis of experimental results and final microstructures lead to the following conclusions.

1. In the clean condition, continuous densification proceeded without evidence for abnormal grain growth up to 1900 °C for 5 hr. The average grain size followed the normal-grain-growth-kinetics law, and the grain shape remained equiaxed.

2. In the normal sintering condition, abnormal grain growth was observed at a lower sintering temperature. However, the densification rate and grain-growth kinetics increased by a factor of 3–5 until abnormal grains appeared suddenly. Once abnormal grain growth occurred, further densification stopped abruptly.

3. Abnormal grain growth in commercial high-purity alumina is *not* an intrinsic property of alumina *but* an extrinsic property controlled by minor constituents that can be introduced during powder synthesis, powder processing and sintering.

4. The effect of impurities is likely to be related to the alteration of interfacial chemistry through preferential segregation to specific grain boundaries or pore surfaces, and the formation of liquid phases which are suspected to be associated with abnormal grain growth in commercial alumina.

5. It is thus necessary to consider the effects of MgO in conjunction with the impurities which are responsible for abnormal grain growth during the final stage of alumina sintering.

Acknowledgements

The authors are grateful for the financial support from the Korean Science and Engineering Foundation (KOSEF) and from the Research Institute of Industrial Science and Technology (RIST).

References

1. R. L. COBLE, *J. Appl. Phys.* **32** (1961) 793.
2. J. G. J. PEELEN, *Mater. Sci. Res.* **10** (1975) 443.
3. S. J. BENNISON and M. P. HARMER, *J. Amer. Ceram. Soc. C* **68** (1985) 22.
4. K. A. BERRY and M. P. HARMER, *ibid.* **69** (1986) 143.
5. T. K. IKEGAMI, K. KOTANI and K. EGUCHI, *ibid.* **70** (1987) 885.
6. W. A. KAYSSER, M. SPRISLER, C. A. HANDWERKER and J. E. BLENDLELL, *ibid.* **70** (1987) 339.
7. C. A. HANDWERKER, P. A. MORRIS and R. L. COBLE, *ibid.* **72** (1989) 130.
8. S. BAIK and J. H. MOON, *ibid.* **74** (1991) 819.
9. P. A. MORRIS, in "Ceramic transactions", Vol. 7, edited by C. A. Handwerker, J. E. Blendell and W. A. Kaysser (American Ceramic Society, Westerville, Ohio, 1990) p. 50.
10. T. SATA and T. SASAMOTO, *Taikabutsu* **34** (1982) 295.
11. P. REIJNEN and H. D. KIM, *Ber. Dtsch. Keram. Ges.* **62** (1986) 272.
12. Y. K. SIMPSON and C. B. CARTER, *J. Amer. Ceram. Soc.* **73** (1990) 2391.
13. S. C. HANSEN and D. S. PHILLIPS, *Phil Mag. A* **47** (1983) 209.
14. D. W. SUSNITZKY and C. B. CARTER, *J. Amer. Ceram. Soc.* **73** (1990) 2485.
15. E. DÖRRE and H. HÜBNER, in "Alumina: Processing, properties, and applications" (Springer-Verlag, Berlin, 1984) p. 16.
16. R. J. BROOK, in "Treatise on materials science and technology", Vol. 9, edited by F. F. Wang (Academic Press, New York, 1976) p. 331.
17. M. P. HARMER, in "Structure and properties of MgO and alumina ceramics", Vol. 10, edited by W. D. Kingery (American Ceramic Society, Westerville, Ohio, 1984) p. 679.
18. W. S. PATRICK and I. B. CUTLER, *J. Amer. Ceram. Soc.* **48** (1965) 541.
19. S. S. KIM and S. BAIK, *Solid State Phenom.* **25-26** (1992) 269.

Received 28 July

and accepted 21 October 1992